Asia-Pacific Journal of Atmospheric Sciences (2022) 58:197–205
https://doi.org/10.1007/s13143-021-00249-y

Online ISSN 1976-7951
Print ISSN 1976-7633

ORIGINAL ARTICLE

Relationship between Arctic Sea Ice in Autumn and Subsequent July Air Temperature over East Asia and the Western North Pacific

Wookap Choi[1] · Simchan Yook[1,2]

Received: 10 March 2021 / Revised: 14 June 2021 / Accepted: 15 June 2021 / Published online: 28 June 2021

Abstract

We investigated the relationship between the Arctic sea ice area and the following year's atmospheric temperature using reanalysis data. The results demonstrate that the July air temperature at 850 hPa, observed over East Asia (EA) and Western North Pacific (WNP), shows a strong correspondence to the Arctic sea-ice area during the previous year's September–November period. This relation has been observed since 2007. A strong relationship between the air temperature and the Arctic sea ice is observed only when the sea ice area in autumn is smaller than approximately 6.3 million km^2. This threshold value coincides with the record reduction in the Arctic sea ice in the autumn of 2007. Sea surface temperature over the Northern Pacific also shows a similar correlation with the Arctic sea ice. The study of these correlations may provide a potential technique for seasonal prediction of July air temperature over EA and the WNP regions.

Keywords Arctic sea ice · Sea-ice reduction · July air temperature · East Asia · Western North Pacific · Prediction

1 Introduction

A substantial amount of Arctic sea ice has melted in recent decades with several record-breaking sea ice area minimums (Stroeve et al. 2012). The melting sea ice plays an important role in Arctic climate change, indicated by the strong positive ice-temperature feedbacks observed in the Arctic region (Screen and Simmonds 2010). Considering the potential links between the Arctic and the midlatitude weathers that are induced by large-scale circulation changes (Cohen et al. 2014), examining the atmospheric responses related to the loss of Arctic sea ice is essential for improving not just our understanding of climate change but also seasonal forecasting. Several studies have suggested the relationship between the recent reduction in the Arctic sea ice and the changes in the atmospheric temperatures and circulations in the midlatitudes. Some of the studies on this topic are as follows: early autumn sea ice and the wintertime Eurasian climate by Honda et al. (2009), the autumn Arctic sea ice on Eurasian spring air temperature (Chen and Wu 2018) and East Asian winter monsoon (Chen et al. 2014), early winter sea ice and mid-winter stratospheric polar vortex by Kim et al. (2014), and Arctic sea-ice loss and recent Eurasian winter cooling by Nakamura et al. (2015) and Mori et al. (2014, 2019). The atmospheric responses to the variations in the Arctic sea ice are complex depending on the background atmospheric state and season (Kug et al. 2015; Overland et al. 2016). Compared to the research carried out on the potential influence of autumnal sea ice on winter atmospheric circulation, the link between the autumnal Arctic sea ice and the atmospheric conditions during the next summer is barely studied.

In the preliminary study, we observed a potential relationship between the area of the Arctic sea ice (during the autumn season) and the July air temperature over the Korean peninsula since 2007. The goal of this study is to identify any other midlatitude region that shows a similar relationship with the Arctic sea ice area. Since the record reduction of Arctic sea ice has been observed in September 2007 (Comiso et al. 2008; Stroeve et al. 2008), the atmospheric conditions observed in recent decades seem to be quite different from those in earlier period. We conducted an observational analysis to understand the temporal and spatial characteristics of the correlation

Responsible Editor: June-Yi Lee.

✉ Wookap Choi
wchoi@snu.ac.kr

[1] School of Earth and Environmental Sciences, Seoul National University, Seoul, Korea

[2] Department of Atmospheric Science, Colorado State University, Fort Collins, CO, USA

observed between the summertime air temperature of the Northern Hemisphere and the previous year's Arctic sea ice area. We do not attempt to address the detailed dynamical mechanisms to account for the linkage. Instead, we focus on documenting the observed signals, which can become a starting point for a more sophisticated analysis. The information on the dataset used in this study is provided in Section 2. In Section 3, relations found between the Arctic sea ice area of one year and the July air temperature of the following year are discussed. This is followed by a summary of our conclusions given in Section 4.

2 Data and Methods

Air temperature for the period of 1979–2020 were obtained from the ERA5 of the European Center for Medium-Range Weather Forecasts (ECMWF) at 0.25° horizontal resolution (Hersbach et al. 2020). Sea ice concentration data corresponding to the same period (1979–2019) was obtained at 0.25° resolution from the Sea Ice Index Version 3 [National Snow and Ice Data Center (NSIDC)] that was consolidated from passive microwave satellite observations (Fetterer et al. 2017). In this study, we calculated the sea ice area (SIA) by summing the area covered by sea ice in the entire Northern Hemisphere; the calculated SIA was used for the analysis. The monthly-mean SIA was averaged to obtain the SIA during the September-October-November (SON) period. This average is henceforth referred to as SON SIA and it is used for all calculations in this study.

For the sea surface temperature (SST) analysis, we used the optimum interpolation sea surface temperature version 2 (OISST V2) data [National Oceanic and Atmospheric Administration (NOAA)] set at 1° horizontal resolution for the period of 1982–2020 (Reynolds et al. 2002). All the regression analyses used in this study are simple linear regression analyses. A standard two-tailed t-test is used for testing the statistical significance of the regression analysis, and a two-tailed f-test is applied to assess the statistical significance of the difference observed in the standard deviation.

3 Results

3.1 Area of the Arctic Sea Ice in Autumn

To determine the most significant relationship between the SIA in SON and the midlatitude air temperature in another month, correlation analyses were performed for air temperatures (at the 850 hPa level) in the Northern Hemisphere for all months by using SON SIA. Large correlations are found between SON SIA and the July air temperature over the Western North Pacific (40–50°N, 150–165°E); strong correlations appear only after 2007. The SIA in SON for the period of 1979–2019 is shown in Fig. 1. The vertical axis in the diagram is inverted to depict the reducing SIA. In Fig. 1 the SIA has been decreasing, showing a trend of -0.71 million km^2 per decade. A dramatic change in SIA occurred in September 2007 in which the Arctic sea ice melted by record amount (Comiso et al. 2008; Stroeve et al. 2008). SON SIA was reduced below the level of 6.3 million km^2 (indicated by the dashed line) in 2007, and never recovered that level until now.

3.2 Correlation between Autumn SIA and July Air Temperature

Figure 2a shows the monthly-mean air temperature at 850 hPa averaged over the region of WNP in July. The air temperature shows that the linear trend in the recent years is small. The interannual variation seems to be decreasing in recent decades. In Fig. 2b, the WNP temperature in July (for the year) is plotted against the SON SIA calculated in the preceding year. The axis of SIA is inverted in Fig. 2b. In the figure, we can observe that there is an increase in the July air temperature corresponding to the decrease in SIA. In this scatter plot some distinct features appear. First of all, there is a transition value of SIA between 6 and 7 million km^2, and the correlation between the temperature and the SIA shows a substantial change across this value. During the year of low SIA (less than 6.3 million km^2), the July air temperature shows a stronger linear relationship with the SIA. In Fig. 1, the years that had lower SIA (less than 6.3 million km^2) appear from 2007 to present. Considering the record melting of Arctic sea ice in 2007 and the information given in Figs. 1 and 2b, we define the periods "PRE" and "POST" dependent on the threshold value of the SIA, which is about 6.3 million km^2. It turns out that the PRE and POST periods correspond to 1979–2006 and 2007–2019, respectively, in terms of the sea ice area. In terms of the air temperature, the PRE and POST periods correspond

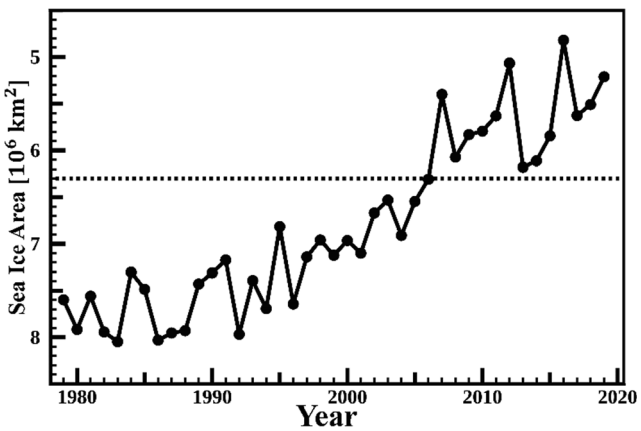

Fig. 1 Area of the Arctic sea ice during SON. Dashed line represents an area of 6.3 million km^2. Vertical axis is inverted for future purposes

to 1980–2007 and 2008–2020, respectively. The numbers in Fig. 2b represent the year of July temperature e.g., the number 08 denotes the air temperature for July 2008 that shows correlation to the SIA of September 2007. In Fig. 2, linear regression line is drawn for each period by a dashed line. The regime shift in the year of 2007 was reported to be associated with the Arctic marine system (Ogi et al. 2016; and references therein). Overland et al. (2012) noted that the period of 2007–2012 showed a persistent change in early summer Arctic wind patterns relative to the previous decades. Also, the six summers from 2007 to 2012 had more precipitation than average over northern Europe (Screen 2013).

As the axis of SIA is inverted in Fig. 2b, the signs of both correlation and regression coefficients are also reversed. The regression coefficients for PRE and POST are 0.12 and 1.17 K per million km^2, respectively. The relationship between the SIA and the air temperature in July shows a large difference between the PRE and the POST periods. Although the time series of air temperature in July given in Fig. 2a shows no statistically significant trend during PRE (at $p = 0.65$) and POST (at $p = 0.54$), the air temperature in July and the SIA during POST (Fig. 2b) shows a statistically significant positive linear relation ($r = 0.65$) at the $p = 0.02$ level. To see the change between the two periods quantitatively in Fig. 2b, the standard deviation is calculated after subtracting the linear regression. In the time series of the air temperature (Fig. 2a), the detrended standard deviation shows a small difference between PRE (1.29 K) and POST (0.88 K). In Fig. 2b, the standard deviation of 1.29 K during PRE decreases to 0.75 K during POST. In other words, the air temperature at 850 hPa might be significantly affected by the Arctic SIA if it reduces to an area less than 6.3 million km^2. This reduction has been observed from 2007 and is ongoing. The temperature values in 2019 and 2020 are somewhat lower than the predicted values by the regression line. Obviously there are other factors controlling the July temperatures in addition to the SON sea ice condition. One of the factors may be local climate such as monsoon. We cannot pinpoint the exact reason for the low July temperatures in 2019 and 2020.

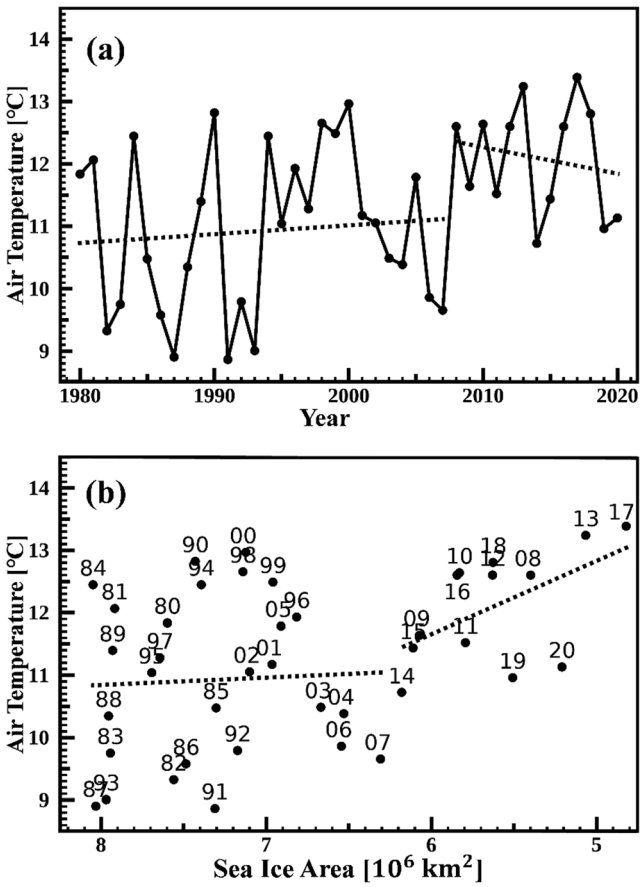

Fig. 2 (**a**) Monthly-mean July air temperature at 850 hPa over WNP with respect to time, and (**b**) scatter plot of SON SIA in the previous year versus July air temperature over WNP. The horizontal axis is inverted. Numbers in (**b**) represent year of temperature. Dashed lines indicate temporal trend in (**a**), and regression lines in (**b**) during PRE and POST periods (as defined in the manuscript)

3.3 Regions of Strong Correlations

Decrease of the standard deviation of air temperature from PRE to POST with respect to the linear regression line indicates that the portion of air-temperature variability explained by SON SIA has increased. During the POST period, since the linear relationship between the SIA and the air temperature in July is strong, SON SIA has the potential for predicting the next year's air temperature for the month of July. For establishing a reliable linear relationship between SIA and air temperature during POST, studying large correlation and regression coefficients as well as small standard deviations is crucial. The question arises whether there are any other regions showing a similar relationship between air temperature and SON SIA. To search for such regions, we used the following three criteria: (1) During POST, the correlation must be statistically significant (at 99 % confidence level), and the regression coefficient must be larger than 1.25 K per million km^2, (2) The standard deviation obtained after subtracting the linear regression between air temperature and SIA must decrease from PRE to POST, and the difference between them must be statistically significant (at 99 % confidence level), and (3) The trend of air temperature with time must be statistically insignificant. If the air temperature in a certain region shows a significant increase with time, the increase might be due to global warming and in such a case, the dependence of the temperature change on the SIA might be uncertain.

3.3.1 Correlations Observed in East Asia and WNP Regions

Correlation coefficients for the whole Northern Hemisphere were calculated for air temperature with SON SIA

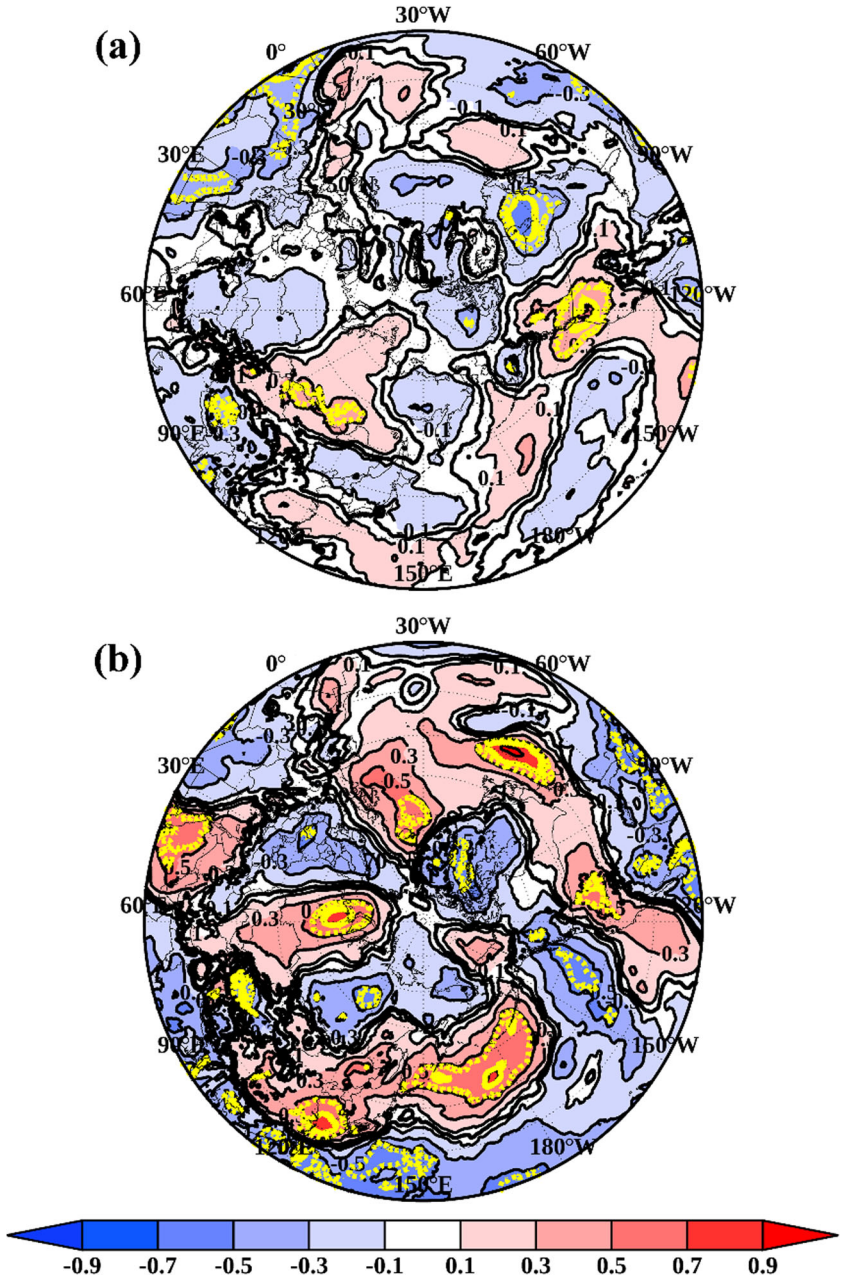

Fig. 3 Correlation coefficients between July air temperature at 850 hPa and SIA in previous SON during (**a**) PRE and (**b**) POST for north of 20°N. The yellow dashed line represents the statistical significance at 95 % while the yellow solid line represents the statistical significance at the 99 % levels. Sign of the coefficients is reversed

corresponding to the PRE and POST periods. The results are shown in Fig. 3, and it shows the correlation coefficients between air temperature in July at 850 hPa north of 20°N and SIA in previous SON. Two areas showing the strongest correlations are East Asia (30–45°N, 120–135°E) and Western North Pacific (40–50°N, 150–165°E). A small region in Nunavut, Canada (75°N, 90°W) satisfies the first criterion (defined in Section 3.3), but has the opposite sign of correlations. Although the second criterion (reduction of the standard deviation), is also satisfied in Nunavut, the third criterion is not. And thus, the dependency of air temperature either on global warming or on the reduction of SIA is uncertain. In the Atlantic Ocean, two regions (located over 60°N, 33°W and 40°N, 60°W) show positive correlations. The small area near 40°N, 60°W satisfies all the three criteria, although the area covered by the positive correlation is much smaller than EA and WNP regions. One thing worthy of noting is that the centers of strong positive correlations are located over the western boundary of both the Pacific and Atlantic Oceans; no centers are located over continents.

In this study, we concentrate on the Pacific region (20–70°N, 100°E–160°W) for analyzing the localized structure of the linear relationships. The signs of the correlations and regression coefficients are also reversed to represent the changes in target variables corresponding to the decrease in

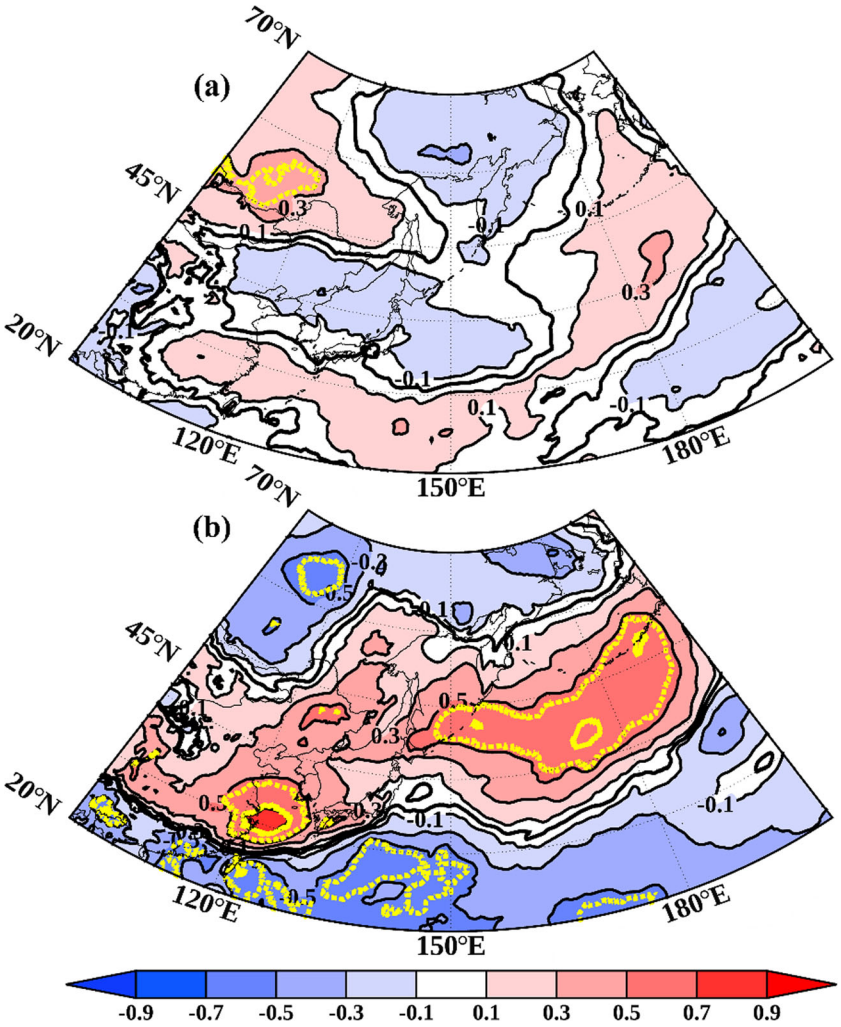

Fig. 4 Correlation coefficients between air temperature in July at 850 hPa and SIA in previous SON period during (**a**) PRE and (**b**) POST periods. The yellow dashed line represents the statistical significance at 95 % while the yellow solid line represents the statistical significance at the 99 % levels. Sign of the coefficients are reversed

SIA. Thus, a positive correlation implies an increase in the air temperature with decreasing SIA. Figure 4 shows the correlation coefficients between air temperature in July at 850 hPa and SIA in previous SON, same as those shown in Fig. 3. In Fig. 4, while there is no area of noticeable correlations in PRE (Fig. 4a), in POST, two areas showing the strongest

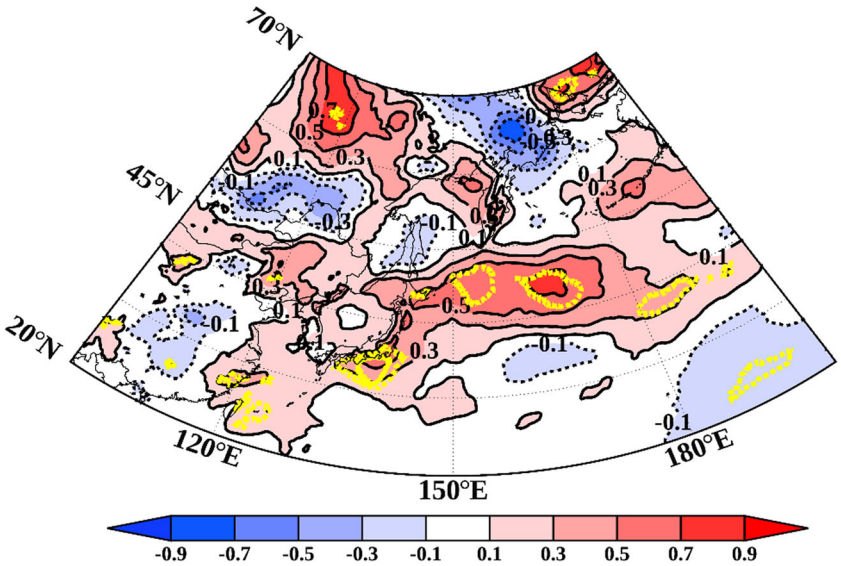

Fig. 5 Difference (PRE minus POST) in the standard deviations of the air temperature in July at 850 hPa (K), calculated after subtracting the linear regression with the SON SIA. The yellow dashed line represents the statistical significance at 95 % while the yellow solid line represents the statistical significance at the 99 % levels

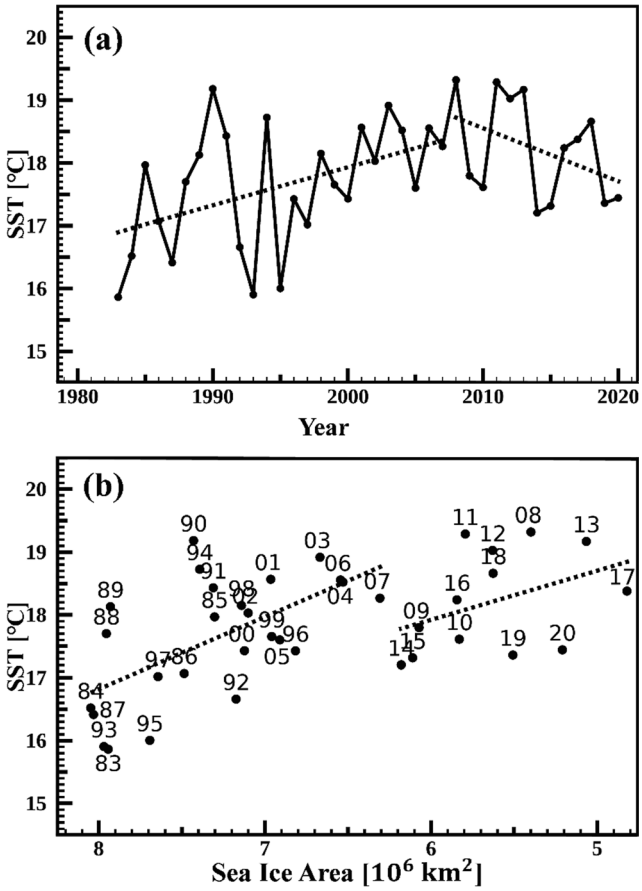

Fig. 6 (**a**) Monthly-mean July SST averaged over 35–45°N, 172.5°E–172.5°W with respect to time, and (**b**) scatter plot of SON SIA in the previous year versus SST in July. The horizontal axis (of SIA) is inverted. Numbers in (**b**) represent year of SST. Dashed lines indicate temporal trend in (**a**), and regression lines in (**b**) during PRE and POST periods

correlation are located in East Asia (30–45°N, 120–135°E) and WNP. During the POST period in Fig. 4b, regions over EA and WNP satisfy all the three criteria described above. In EA and WNP, two centers that show distinct positive correlations are located along the western boundary of the Pacific Ocean having a maximum value of 0.74 at 31.5°N, 124.5°E, and 0.69 at 43.0°N, 172.0°E (Fig. 4b). The regions that show a significant decrease in the standard deviations from PRE to POST are given in Fig. 5. The regions located in WNP and EA overlap with the areas of strong correlations. In addition to the statistically significant correlations observed, the decrease in the standard deviation implies that the SIA from the previous SON period, can be used to predict the air temperature in July for the following year.

3.3.2 Correlations with Sea Surface Temperature

The linear relationships established over a wide area may indicate the existence of time-lagged connections between the Arctic sea-ice region and the large-scale atmospheric variability in July witnessed over the Western Pacific region. The time-delay between the SIA and the July air temperature is about nine months, which is substantial considering the typical duration of the dynamical memory of atmosphere. In contrast to the atmosphere, the memory of oceans is much longer, and thus, the ocean may play a key role determining the influence of autumn Arctic sea ice on the air temperature over the Pacific Ocean nine months later. As suggested by Wills and Thompson (2018), variations in the SSTs in the midlatitude oceans are capable of significantly influencing large-scale atmospheric circulations, especially near the western boundary currents.

To investigate the variation of SST (Fig. 6) with the reduction in Arctic SIA and its impact on the atmospheric circulation, we calculated the correlation coefficients between the SIA and the SST fields over the same region (Fig. 7). For the SST data, the PRE period starts from 1983 due to the limited data available. The difference in the standard deviations is shown in Fig. 8. Areas that show significant correlations with respect to the SST (bottom panel of Fig. 7) are located close to the areas that show strong correlations with respect to the air temperature (Fig. 4b). However, the areas that show strong SST correlations are located towards the south when compared to the areas that show strong air-temperature correlations. Correlation coefficients were calculated for SST in every month. In the preceding months, May and June, SST correlations were not so strong as that in July (figure not shown).

Investigating the detailed physical mechanism behind the sea-air interaction, including the accurate lead-lag relationship between the SST and the air temperature, is beyond the scope of this paper. However, considering the vertical structure of the atmospheric response seen over the WNP region, the regression map is shown in Fig. 9 instead of the correlation map to indicate the effect of SIA variation on temperature response. Significant warming is observed between 1000 hPa and 700 hPa over 40–50°N. The atmospheric circulation response is not limited to the lower levels of the troposphere but reveals a barotropically-developed vertical structure extending from the surface of the earth to the upper troposphere over the WNP region. The contour lines of the centers of positive regressions located between the levels of 1000 hPa and 700 hPa over 40–50°N, slope upwards towards the north direction, consistent with the southward difference of the locations of the positive center in the horizontal SST and air temperature correlation maps. We suspect that the correlation patterns observed between SST and air temperature may not be a coincidence but a possible influence of SST on the atmosphere.

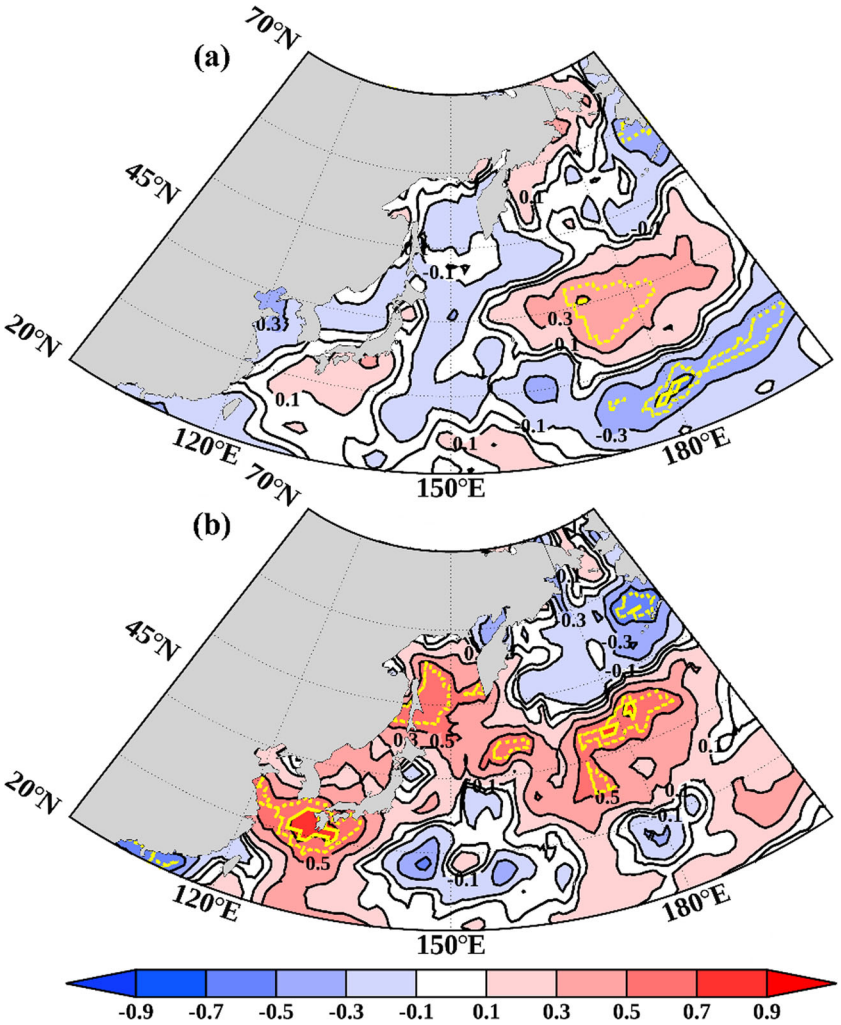

Fig. 7 Correlation coefficients between the July SST and the SIA in previous SON period during (top) PRE and (bottom) POST periods. The yellow dashed line represents the statistical significance at 95 % while the yellow solid line represents the statistical significance at the 99 % levels. Sign of the coefficients are reversed

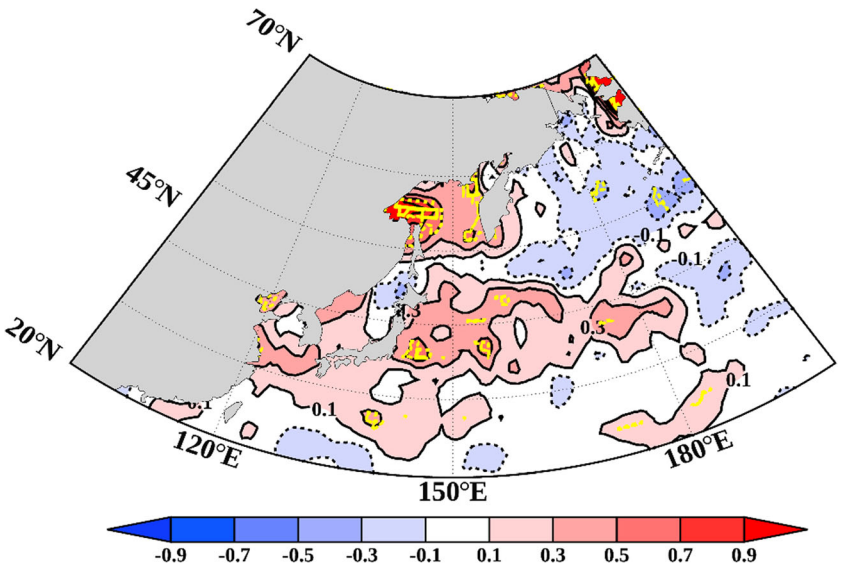

Fig. 8 Difference (PRE minus POST) of the standard deviations of the July SST (K), calculated after subtracting the linear regression with SON SIA. The yellow dashed line represents the statistical significance at 95 % while the yellow solid line represents the statistical significance at the 99 % levels

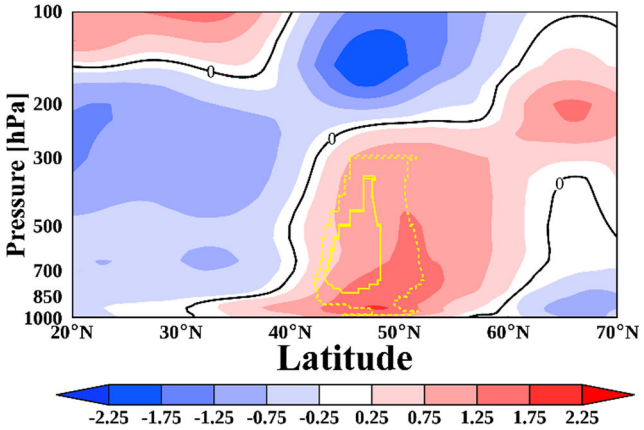

Fig. 9 Latitude-height cross section of air temperature in July regressed on SON SIA (K per million km^2), averaged over 150°E–150°W. The black solid contour line has a regression of zero. Sign of the regression coefficients is reversed, and thus, positive values represent warming after decrease in SIA

4 Summary and Discussions

We have investigated the possible connections between the autumnal Arctic sea ice area and the summertime extratropical air temperature over EA and WNP using an observational dataset. A strong linear relationship between them appears after 2007 in corresponding to the record reduction of the Arctic sea ice that occurred in September 2007. This reduction of sea ice in 2007 resulted in the regime shift; the resulting atmospheric and marine conditions were reported by several studies (Comiso et al. 2008; Ogi et al. 2016; Overland et al. 2012; Screen 2013; Stroeve et al. 2008). This regime shift corresponds to a specific threshold value of the SIA, which is about 6.3 million km^2 in the SON period. After 2007, SON SIA never exceeded that value.

The midlatitude temperature at 850 hPa in July in Northern Hemisphere is more strongly related with the Arctic SIA during POST than during PRE (Fig. 3). Distinctive linear relations between the July air temperature over EA and WNP and SON SIA, are identified during POST (Fig. 4) with the decrease in the standard deviations of the air temperature calculated after subtracting the linear regressions (Fig. 5). The correlation map of SST has shown similar correlations with air temperature at 850 hPa, with a small difference seen in the location of the positive center over WNP (southward direction).

Although we did not investigate the dynamical relationship between the SON SIA and the SST in July, the coherent patterns in the correlation maps seen between SST and air temperature (dependent on SIA) might offer a small clue indicating the link between the autumnal Arctic sea-ice loss and the atmospheric circulation in summer. Our hypothesis for deducing the dynamic pathway of the July temperature-change related to sea-ice reduction in the Arctic is as follows: Reduction of the Arctic sea ice below the threshold value of 6.3 million km^2 could help enhance the mobility of Arctic sea water, and the resulting change in ocean currents leads to a freer movement of the Arctic sea water into the Pacific Ocean. After nine months, SST in some Pacific regions might be affected by the changes in ocean currents such as the Oyashio and Kuroshio currents. And finally, air temperature follows the change in SST because SST variations are capable of influencing the atmospheric circulation (Wills and Thompson 2018). Regarding the important roles played by air temperature and SST in determining the climate in July, our study suggests the possibility of using data of the Arctic sea ice (in autumn) for seasonal forecasting for the month of July in the consecutive year for East Asia and Western North Pacific regions. In addition, we are going to investigate the role of certain specific regions rather than the entire Arctic domain, since responses to regional and pan-Arctic sea ice anomalies are different in model results (Screen 2017).

Acknowledgements We thank Prof. Kwang-Y. Kim for his help on revising the manuscript. Further analyses of data by Young-Ah Kim and Jungjin Kim are greatly appreciated. This work was supported by the National Research Foundation of Korea (2018R1A2B6003197).

Funding Funding authority: National Research Foundation of Korea, Grant number: 2018R1A2B6003197.

Data Availability The ERA5 reanalysis data were downloaded from https://cds.climate.copernicus.eu/cdsapp#!/home website. Satellite-observed sea ice concentration data are provided by NSIDC (http://nsidc.org/data/seaice/). The OISST V2 data sets are downloaded from https://www.emc.ncep.noaa.gov/research/cmb/sst_analysis/ website.

Code Availability Not applicable.

Declarations

Conflict of Interest Not applicable.

References

Chen, Z., Wu, R., Chen, W.: Impacts of autumn Arctic sea ice concentration changes on the East Asian winter monsoon variability. J. Clim. **27**(14), 5433–5450 (2014)

Chen, S., Wu, R.: Impacts of early autumn Arctic sea ice concentration on subsequent spring Eurasian surface air temperature variations. Clim. Dyn. **51**(7–8), 2523–2542 (2018)

Cohen, J., Screen, J.A., Furtado, J.C., Barlow, M., Whittleston, D., Coumou, D., Francis, J., Dethloff, K., Entekhabi, D., Overland, J.: Recent Arctic amplification and extreme mid-latitude weather. Nat. Geosci. **7**(9), 627–637 (2014)

Comiso, J.C., Parkinson, C.L., Gersten, R., Stock, L.: Accelerated decline in the Arctic sea ice cover. Geophys. Res. Lett. **35**(1) (2008)

Fetterer, F., Knowles, K., Meier, W., Savoie, M., Windnagel, A.: Updated daily. Sea ice index, version 3. National Snow and Ice Data Center (NSIDC), Boulder (2017)

Hersbach, H., Bell, B., Berrisford, P., et al.: The ERA5 global reanalysis. Q. J. R. Meteorol. Soc. **146**, 1999–2049 (2020)

Honda, M., Inoue, J., Yamane, S.: Influence of low Arctic sea-ice minima on anomalously cold Eurasian winters. Geophys. Res. Lett. **36**(8) (2009)

Kim, B.-M., Son, S.-W., Min, S.-K., Jeong, J.-H., Kim, S.-J., Zhang, X., Shim, T., Yoon, J.-H.: Weakening of the stratospheric polar vortex by Arctic sea-ice loss. Nat Commun **5**(1), 1–8 (2014)

Kug, J.-S., Jeong, J.-H., Jang, Y.-S., Kim, B.-M., Folland, C.K., Min, S.-K., Son, S.-W.: Two distinct influences of Arctic warming on cold winters over North America and East Asia. Nat. Geosci. **8**(10), 759–762 (2015)

Mori, M., Watanabe, M., Shiogama, H., Inoue, J., Kimoto, M.: Robust Arctic sea-ice influence on the frequent Eurasian cold winters in past decades. Nat. Geosci. **7**(12), 869–873 (2014)

Mori, M., Kosaka, Y., Watanabe, M., Nakamura, H., Kimoto, M.: A reconciled estimate of the influence of Arctic sea-ice loss on recent Eurasian cooling. Nat. Clim. Chang. **9**(2), 123–129 (2019)

Nakamura, T., Yamazaki, K., Iwamoto, K., Honda, M., Miyoshi, Y., Ogawa, Y., Ukita, J.: A negative phase shift of the winter AO/NAO due to the recent Arctic sea-ice reduction in late autumn. J. Geophys. Res. Atmos. **120**(8), 3209–3227 (2015)

Ogi, M., Rysgaard, S., Barber, D.G.: Importance of combined winter and summer Arctic Oscillation (AO) on September sea ice extent. Environ. Res. Lett. **11**(3), 034019 (2016)

Overland, J.E., Francis, J.A., Hanna, E., Wang, M.: The recent shift in early summer Arctic atmospheric circulation. Geophys. Res. Lett. **39**(19) (2012)

Overland, J.E., Dethloff, K., Francis, J.A., Hall, R.J., Hanna, E., Kim, S.-J., Screen, J.A., Shepherd, T.G., Vihma, T.: Nonlinear response of mid-latitude weather to the changing Arctic. Nat. Clim. Chang. **6**(11), 992–999 (2016)

Reynolds, R.W., Rayner, N.A., Smith, T.M., Stokes, D.C., Wang, W.: An improved in situ and satellite SST analysis for climate. J. Clim. **15**(13), 1609–1625 (2002)

Screen, J.A., Simmonds, I.: The central role of diminishing sea ice in recent Arctic temperature amplification. Nature **464**(7293), 1334–1337 (2010)

Screen, J.A.: Influence of Arctic sea ice on European summer precipitation. Environ. Res. Lett. **8**(4), 044015 (2013)

Screen, J.A.: Simulated atmospheric response to regional and pan-Arctic sea ice loss. J. Clim. **30**, 3945–3962 (2017)

Stroeve, J., Serreze, M., Drobot, S., Gearheard, S., Holland, M., Maslanik, J., Meier, W., Scambos, T.: Arctic sea ice extent plummets in 2007. Eos, Trans. Am. Geophys. Union **89**(2), 13–14 (2008)

Stroeve, J.C., Serreze, M.C., Holland, M.M., Kay, J.E., Malanik, J., Barrett, A.P.: The Arctic's rapidly shrinking sea ice cover: a research synthesis. Clim. Change **110**(3), 1005–1027 (2012)

Wills, S.M., Thompson, D.W.: On the observed relationships between wintertime variability in Kuroshio–Oyashio Extension sea surface temperatures and the atmospheric circulation over the North Pacific. J. Clim. **31**(12), 4669–4681 (2018)